

# Detection of catechol using mixed Langmuir–Blodgett films of a phospholipid and phthalocyanines as voltammetric sensors

Priscila Alessio,<sup>abc</sup> Felipe J. Pavinatto,<sup>bd</sup> Osvaldo N. Oliveira Jr.,<sup>\*d</sup> Jose Antonio De Saja Saez,<sup>c</sup> Carlos J. L. Constantino<sup>a</sup> and Maria Luz Rodríguez-Méndez<sup>b</sup>

Received 17th March 2010, Accepted 9th July 2010

DOI: 10.1039/c0an00159g

The combination of metallic phthalocyanines (MPcs) and biomolecules has been explored in the literature either as mimetic systems to investigate molecular interactions or as supporting layers to immobilize biomolecules. Here, Langmuir–Blodgett (LB) films containing the phospholipid dimyristoyl phosphatidic acid (DMPA) mixed either with iron phthalocyanine (FePc) or with lutetium bisphthalocyanine (LuPc<sub>2</sub>) were applied as ITO modified-electrodes in the detection of catechol using cyclic voltammetry. The mixed Langmuir films of FePc + DMPA and LuPc<sub>2</sub> + DMPA displayed surface-pressure isotherms with no evidence of molecular-level interactions. The Fourier Transform Infrared (FTIR) spectra of the multilayer LB films confirmed the lack of interaction between the components. The DMPA and the FePc molecules were found to be oriented perpendicularly to the substrate, while LuPc<sub>2</sub> molecules were randomly organized. The phospholipid matrix induced a remarkable electrocatalytic effect on the phthalocyanines; as a result the mixed LB films deposited on ITO could be used to detect catechol with detection limits of  $4.30 \times 10^{-7}$  and  $3.34 \times 10^{-7}$  M for FePc + DMPA and LuPc<sub>2</sub> + DMPA, respectively. Results from kinetics experiments revealed that ion diffusion dominated the response of the modified electrodes. The sensitivity was comparable to that of other non-enzymatic sensors, which is sufficient to detect catechol in the food industry. The higher stability of the electrochemical response of the LB films and the ability to control the molecular architecture are promising for further studies with incorporation of biomolecules.

## Introduction

The control of molecular architectures afforded by techniques such as the Langmuir–Blodgett (LB)<sup>1–3</sup> and electrostatic layer-by-layer (LbL) films<sup>4,5</sup> has led to the development of prototypical organic devices where synergy is achieved by combining distinct materials, including organic–inorganic hybrids.<sup>6–8</sup> The main features of such films exploited in this context are the molecular interactions that are easily tunable owing to the layer-by-layer organization and the ability to preserve the activity of biomolecules. Indeed, because LB and LbL films are produced under mild conditions and with water entrained in the films even after drying, a large number of biomolecules have been successfully immobilized, especially to produce biosensors.<sup>9–11</sup>

Among the many biosensors built with nanostructured films, there have been some dedicated to phenolic compounds<sup>12–14</sup> which are partly responsible for self-oxidation stability and organoleptic characteristics, and are interesting for their use in anti-ageing healthcare products and in the food industry due to their antioxidant activity.<sup>15,16</sup> Other uses for these non-enzymatic

antioxidants include neurological and heart treatments, pesticides and disinfectants.<sup>17,18</sup> This latter use involves high toxicity, therefore requiring stringent control to reduce impacts on the environment.<sup>19</sup> In addition to biosensors, sensing units with no specific interaction with phenolic compounds have also been developed.<sup>20–24</sup> The aim is generally to obtain sensors with a higher stability over time and lower cost than the biosensors, though there is the inevitable decrease in sensitivity because the units are not capable of molecular recognition.

In this study, we propose a platform that can lead to sensing with both specific (*i.e.* biosensors) and non-specific interactions, based on electrochemical measurements. We describe the fabrication of Langmuir–Blodgett (LB) films made with electroactive phthalocyanines in a non-electroactive phospholipid matrix. The rationale is to produce non-enzymatic sensors for phenols, but in a system that is suitable for future immobilization of enzymes. Furthermore, LB films are thinner, more uniform than cast films, for instance, which are advantageous for rapid and reliable responses in sensing. The choice of dimyristoyl phosphatidic acid (DMPA) as the phospholipid was motivated by its ability to produce multilayer LB films and serve as matrix for immobilization of enzymes with preserved activity.<sup>25</sup> The selection of metallo phthalocyanines as the electroactive materials, in its turn, was inspired in extensive work in sensing units, particularly with the advantage of tailoring their properties by changing the central metal atoms.<sup>26</sup> Indeed, metallo phthalocyanines have been combined with phospholipids and amino acids in sensing units.<sup>26,27</sup> Here, in a proof-of-concept experiment we tested phthalocyanine + DMPA LB films to detect catechol, one of the

<sup>a</sup>Faculdade de Ciências e Tecnologia, Unesp Univ Estadual Paulista, 19060-900 Presidente Prudente, SP, Brazil

<sup>b</sup>E.T.S. Ingenieros Industriales, Universidad de Valladolid, 47011 Valladolid, Spain

<sup>c</sup>Facultad de Ciencias, Universidad de Valladolid, 47011 Valladolid, Spain

<sup>d</sup>Universidade de São Paulo, Instituto de Física de São Carlos, Av. Trabalhador São Carlense 400, CP 369, São Carlos, São Paulo, 13566-590, Brazil. E-mail: chu@ifsc.usp.br; Fax: +55 16 3373-9825; Tel: +55 16 3373-9825

most important phenolic compounds which occurs naturally in fruits and vegetables and can be released to the environment during industrial processing. Furthermore, we provide the characterization of the mixed Langmuir films used to transfer onto the solid substrates, as the identification of molecular-level interactions is key to optimizing sensing performance.

## Experimental procedures

### Langmuir and LB films

Langmuir films were produced using a KSV 2000 trough equipped with a Wilhelmy plate. DMPA from Aldrich ( $614.8 \text{ g mol}^{-1}$ ) was dissolved in 70% chloroform and 30% methanol at a concentration of  $0.70 \text{ mg mL}^{-1}$ . FePc from Kodak ( $568.4 \text{ g mol}^{-1}$ ) and LuPc<sub>2</sub> ( $1200 \text{ g mol}^{-1}$ ) synthesized as described in ref. 28 and<sup>29</sup> were dissolved in chloroform at  $0.50$  and  $1.55 \text{ mg mL}^{-1}$ , respectively. The molecular structures of FePc, LuPc<sub>2</sub> and DMPA are shown in Fig. 1. The mixed FePc + DMPA and LuPc<sub>2</sub> + DMPA solutions were prepared by mixing the neat stock solutions to obtain 1 : 1 molar ratio. The mixed solution was gently spread onto a phosphate buffer subphase ( $0.01 \text{ M}$  with NaCl  $0.1 \text{ M}$ ), which was prepared using ultrapure water ( $18.3 \text{ M}\Omega \text{ cm}$ , EASYpure RF) and kept at room temperature ( $22 \text{ }^\circ\text{C}$ ). After spreading the solutions, 15 minutes elapsed for allowing the solvent to evaporate. Then, the Langmuir film was formed by symmetrical compression at  $10 \text{ mm min}^{-1}$ . Though one cannot fabricate LB films from neat LuPc<sub>2</sub>, pure Langmuir monolayers of each material (FePc, LuPc<sub>2</sub> and DMPA) were studied for comparisons.

The LB films were produced by transferring the Langmuir monolayers from the air/water interface onto solid substrates keeping the surface pressure at  $40 \text{ mN m}^{-1}$ . The monolayers were transferred only during the upstroke leading to Z-type LB films. The speed of the dipper varied from  $8 \text{ mm min}^{-1}$  for the first layers to  $0.5 \text{ mm min}^{-1}$  for the last ones to keep the transfer ratio (TR) close to 1. LB films were deposited onto quartz plates for UV-Vis absorption spectroscopy (up to 10 layers), onto Ge for the FTIR measurements (20 layers) and onto ITO for cyclic voltammetry (10 layers). The UV-Vis absorption spectra were recorded with a Shimadzu UV-1603 spectrophotometer and the

FTIR spectra were collected with a Nicolet model Magn IR760 spectrometer.

### Electrochemical characterization and application in sensing

The cyclic voltammetry data were obtained with an EG&G PARC 263A potentiostat/galvanostat (M270 Software) with a conventional three-electrode cell. The reference electrode was a Ag|AgCl/KCl  $3 \text{ mol L}^{-1}$  electrode and the counter electrode was a platinum plate. Cast and LB films were initially immersed into a  $0.1 \text{ M}$  KCl aqueous solution and the cyclic voltammograms were recorded with a scan rate at  $0.1 \text{ V s}^{-1}$ . A kinetic study was also carried out using a  $0.1 \text{ M}$  KCl aqueous solution for the LB films with the scan rate varying from  $0.005$  to  $0.500 \text{ V s}^{-1}$ . For the detection measurements, catechol (Panreac, >99%) was added to the  $0.1 \text{ M}$  KCl aqueous solution at several steps leading to concentrations from  $2.0 \times 10^{-6}$  up to  $2.75 \times 10^{-4} \text{ M}$ . The cyclic voltammograms were recorded from  $-1.0$  up to  $+1.0 \text{ V}$  at a scan rate of  $0.1 \text{ V s}^{-1}$ , and starting at  $0.0 \text{ V}$ . The chemical structure of the analyte catechol is also shown in Fig. 1.

## Results and discussion

### Langmuir films

Fig. 2 shows the  $\pi$ - $A$  isotherms for neat and mixed (1 : 1 mol) Langmuir films recorded at  $22 \text{ }^\circ\text{C}$  using a phosphate buffer ( $\text{pH} = 7.0$  and  $0.01 \text{ M}$ ) with NaCl ( $0.1 \text{ mM}$ ) as subphase, with the mean molecular areas in the  $x$ -axis. This subphase was used because it provides the best environment for most of the enzymes that might be further explored in biosensors. The 1 : 1 molar ratio was chosen as it allows for the incorporation of the biologically relevant DMPA without compromising the catalytic properties of the mixed LB films. Extrapolated areas can be obtained by extrapolating the condensed phase of the  $\pi$ - $A$  isotherms to the  $x$ -axis ( $\pi = 0$ ), as indicated in Fig. 2 by the dashed lines. For neat DMPA, this area was  $46 \text{ \AA}^2$ , in good agreement with the literature for the subphase composition and temperature.<sup>30-32</sup> With such an area the DMPA molecules are mainly arranged perpendicularly to the subphase surface, as

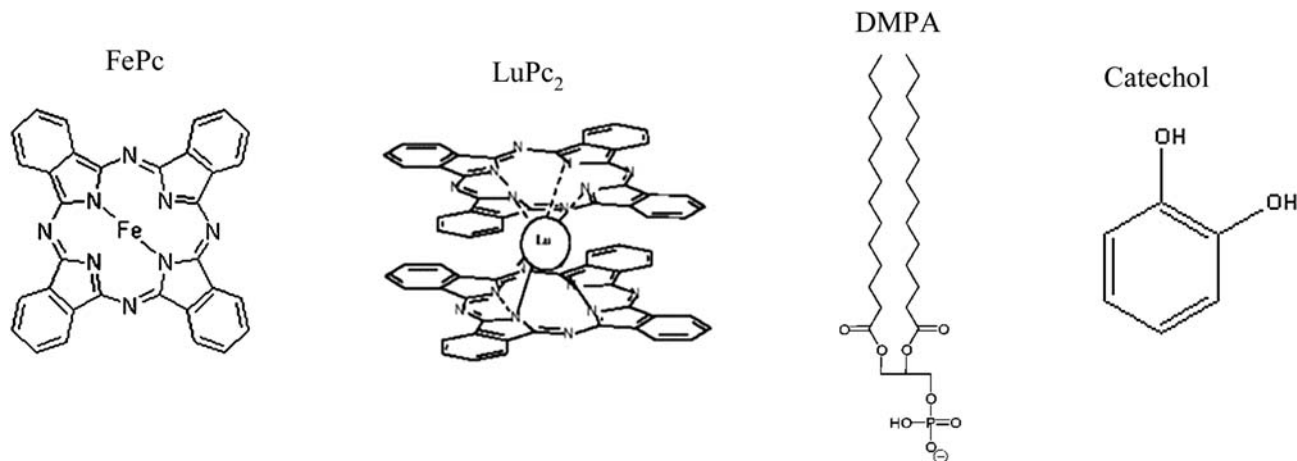
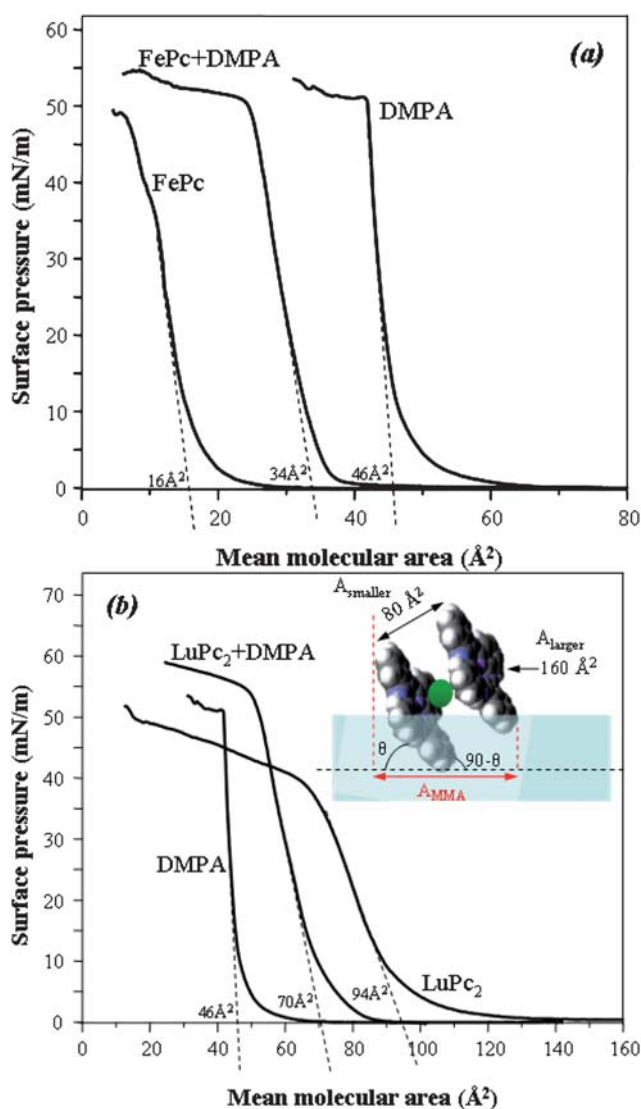


Fig. 1 Molecular structures of FePc, LuPc<sub>2</sub>, DMPA and catechol.



**Fig. 2**  $\pi$ - $A$  isotherms for Langmuir films at 22 °C using a phosphate buffer (pH = 7.0 and 0.1 M) with NaCl (0.1 mM) as subphase. (a) FePc, DMPA and mixed FePc + DMPA (1 : 1 mol); (b) LuPc<sub>2</sub>, DMPA and LuPc<sub>2</sub> + DMPA (1 : 1 mol). The inset in (b) shows the LuPc<sub>2</sub> geometry parameters and a possible molecular organization on the water subphase.

indicated in the literature that suggests a highly ordered hexagonal arrangement.<sup>33</sup>

The molecular arrangement of the phthalocyanine molecules is more difficult to determine. The area per molecule occupied in condensed films is known to depend on the metal of the Pc macrocycle, on the solution solvent and concentration, and on experimental conditions such as subphase temperature and compression rate. For instance, for single macrocycle phthalocyanines, extrapolated areas of 42.8 and 56 Å<sup>2</sup> were found for CuPc<sup>34,35</sup> while for MgPc and PbPc the values quoted were 40 Å<sup>2</sup> and 20 Å<sup>2</sup>, respectively.<sup>36</sup> For FePc, a face-on orientation should lead to an extrapolated area of 160–170 Å<sup>2</sup>, which corresponds to the macrocycle cross section.<sup>37–39</sup> Therefore, the measured 16 Å<sup>2</sup> in Fig. 2a means that the FePc molecules could adopt an almost edge-on orientation, tilted by 85° with the subphase surface ( $\theta = 85^\circ$ ) if we take the extrapolated area as the projection

( $A_{\text{MMA}} = A \cos \theta$ ), where  $\theta$  is the angle between the surface and the plane containing the FePc rings. Another possibility is the stacking of FePc molecules, for an aggregate with 10 molecules in a face-on orientation would also lead to an extrapolated area of 16 Å<sup>2</sup>. However, when the data for deposited LB films are analyzed, we show that the hypothesis of an almost edge-on orientation is the most likely.

The extrapolated area for bisphthalocyanines, e.g. LuPc<sub>2</sub>, is expected to be *ca.* 80 Å<sup>2</sup> for the edge-on orientation under the assumption that the phenyl groups of neighboring molecules interlock.<sup>38,39</sup> One may then assume that the extrapolated area is given by  $A_{\text{MMA}} = A_{\text{larger}} \cos \theta + A_{\text{smaller}} \cos (90 - \theta)$ , where  $A_{\text{larger}} = 160 \text{ \AA}^2$ ,  $A_{\text{smaller}} = 80 \text{ \AA}^2$ . Taking the experimental  $A_{\text{MMA}} = 94 \text{ \AA}^2$  (see inset in Fig. 2b), the tilted angle for a single LuPc<sub>2</sub> molecule would be *ca.* 85°. Interestingly, within the experimental accuracy this value is the same found for a FePc molecule, with an edge-on orientation. The comparison with the literature is not straightforward though, since discrepant values have been reported for bisphthalocyanines. Extrapolated areas were 75 Å<sup>2</sup> for PrPc<sub>2</sub>,<sup>40</sup> 74 Å<sup>2</sup> for YbPc<sub>2</sub>,<sup>41</sup> and 80 Å<sup>2</sup> for LuPc<sub>2</sub> itself, albeit under experimental conditions different from those used here.<sup>38</sup>

In the mixed Langmuir films, the collapse pressure was higher than for the monolayers of the neat compounds, thus denoting an interaction that tended to stabilize the film. However, molecular level interaction was probably very weak as the extrapolated areas were nearly the same as the average between the DMPA and the phthalocyanine neat monolayers. Therefore, the molecular arrangement of both molecules was preserved as in the neat monolayers. A similar result was reported by Clavijo *et al.*<sup>38</sup> for stearic acid + LuPc<sub>2</sub> Langmuir films, while stearic acid was found to induce a significant rearrangement in TiOPc.<sup>42</sup> The central atoms of the Pc seem to play a more important role in the Pc molecular orientation at the air/water interface than the matrix of fatty acid or phospholipid molecules, and this is a subject under current investigation in our labs.

### LB films

Fig. 3 shows the UV-Vis absorption spectra for mixed LB films up to 10 layers deposited onto quartz plates and mixed solutions of (a) FePc + DMPA and (b) LuPc<sub>2</sub> + DMPA. Both MPcs display the characteristic B and Q bands at lower and higher wavelengths, respectively, assigned to  $\pi$ - $\pi^*$  transitions.<sup>43</sup> For LuPc<sub>2</sub>, a band appears at 914 nm, which is assigned to the radical character of the LuPc<sub>2</sub>.<sup>44</sup>

The spectra for FePc in solution and in an LB film are very similar in terms of both the peak position and the band width, indicating the same level of aggregation, consistent with the literature.<sup>45</sup> In contrast, the UV-Vis absorption spectrum of the LuPc<sub>2</sub> solution is blue shifted and better resolved than the spectrum for the LB film, thus pointing to a larger extent of aggregation in the LB film. According to Rodríguez-Méndez *et al.*<sup>44</sup> the red shift in the LB film is caused by J-aggregates in head-to-tail arrangement of transition dipoles in the film.

The linear dependence of the absorbance values at 776 nm and 669 nm in the insets in Fig. 3a and b, respectively, indicates that both mixed LB films grow homogeneously in terms of the amount of MPc deposited per layer. Also observed is that the

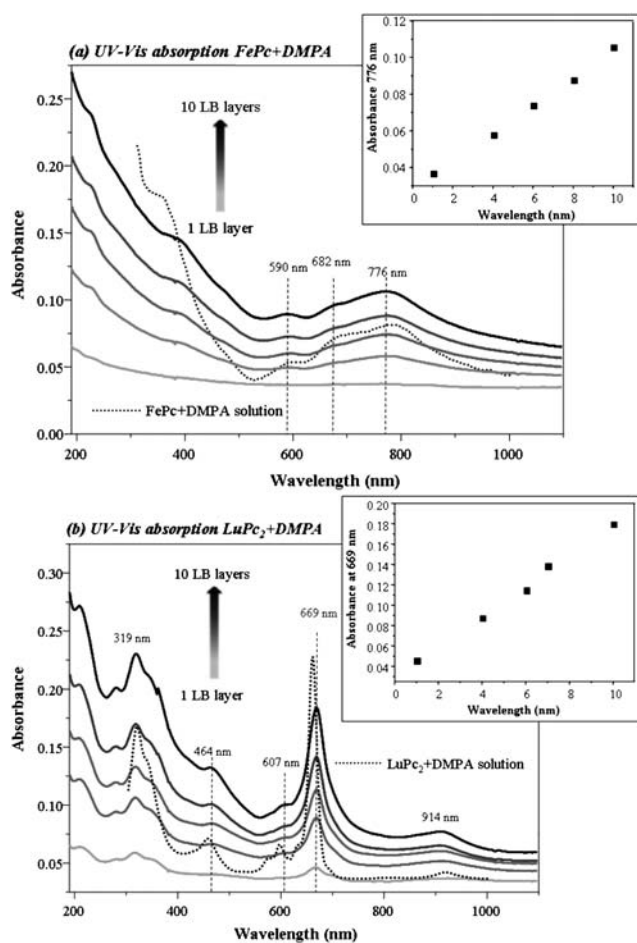


**Fig. 3** UV-Vis absorption spectra for (a) FePc + DMPA and (b) LuPc<sub>2</sub> + DMPA mixed LB films up to 10 layers deposited onto quartz plates. The dashed lines correspond to the mixed solutions.

absorbance of the mixed LB films is higher for LuPc<sub>2</sub> + DMPA for the same number of deposited layers. Therefore, one could speculate that a higher mass of LuPc<sub>2</sub> could be transferred per deposited layer, in comparison to FePc. However, in subsidiary experiments we verified that the extinction coefficient for the Q bands is higher for LuPc<sub>2</sub>. Since correlating quantitatively the absorbance with the mass adsorbed is not straightforward in this case because the materials are different, with distinct spectra, one cannot infer whether the amount of adsorbed film is higher for either MPC.

Fig. 4 shows the FTIR for mixed cast films and 20-layer mixed LB films deposited onto Ge containing (a) FePc + DMPA and (b) LuPc<sub>2</sub> + DMPA. The cast films for the neat materials are given as references. The bands between 1000 and 1200 cm<sup>-1</sup>, at 1465 cm<sup>-1</sup> and between 2800 and 3000 cm<sup>-1</sup>, confirm that DMPA was transferred onto the substrates with either FePc or LuPc<sub>2</sub>. The DMPA bands at 2917 and 2850 cm<sup>-1</sup> are assigned to antisymmetric and symmetric CH<sub>2</sub> stretchings, respectively. The shoulder at 2954 cm<sup>-1</sup> is assigned to antisymmetric CH<sub>3</sub> stretchings, the band at 1738 cm<sup>-1</sup> is assigned to the carbonyl group stretching while that at 1465 cm<sup>-1</sup> is assigned to CH<sub>2</sub> scissoring. The bands at 1171 and 1070 cm<sup>-1</sup> for the DMPA cast film are assigned to antisymmetric and symmetric PO<sub>2</sub><sup>-</sup> stretchings, respectively.<sup>46</sup> The similarity with the spectrum reported by Lozano *et al.*,<sup>47</sup> who showed that the

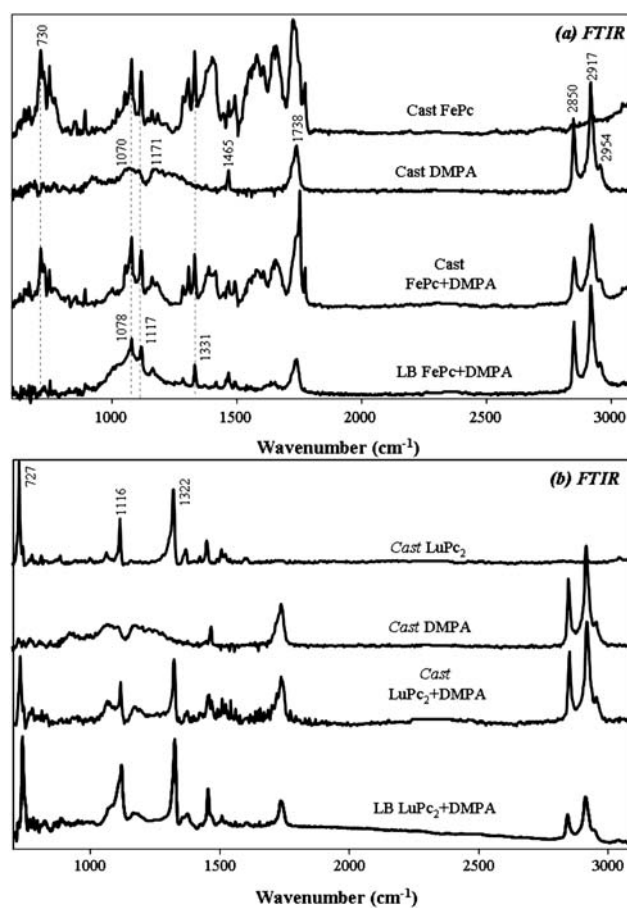


**Fig. 4** FTIR spectra for (a) FePc + DMPA and (b) LuPc<sub>2</sub> + DMPA mixed cast and 20-layer LB films deposited onto Ge plates. The cast films for the neat materials are given as references.

phospholipid molecules are perpendicular to the substrate surface, indicates that the organization of the DMPA molecules in the LB film was not affected by the MPCs, being preserved upon transfer onto a solid support as in the Langmuir film. This is consistent with the lack of interaction inferred from the isotherms of the mixed Langmuir films.

A comparison between the FTIR spectra of neat and mixed samples allows one to obtain two types of information: (i) the possible molecular-level interactions between DMPA and MPCs in the mixed films and (ii) the molecular organization in the mixed LB films assuming that in the cast films the molecules are randomly arranged.

The similarity between the spectra of cast and LB mixed films of LuPc<sub>2</sub> + DMPA in Fig. 4b indicates that the LuPc<sub>2</sub> molecules are randomly organized in the LB films. The LuPc<sub>2</sub> FTIR spectrum is dominated by the bands at 727, 1116 and 1322 cm<sup>-1</sup> assigned to C–H wagging, C–H bending and isoindole stretching, respectively.<sup>48</sup> Furthermore, the FTIR spectra for cast and LB mixed films of LuPc<sub>2</sub> + DMPA are a simple superposition of the spectra of the neat materials. The latter points to a lack of interaction between DMPA and LuPc<sub>2</sub>, which is again consistent with the results from the  $\pi$ -A isotherms in Fig. 2b. Similar results in terms of the isotropy found for the arrangement of LuPc<sub>2</sub> were reported by Aroca *et al.* for thermally vacuum evaporated films (PVD)<sup>49</sup> and LB films of substituted LuPc<sub>2</sub>.<sup>50</sup>

For FePc, Fig. 4a shows that the spectrum of a mixed cast film of DMPA and FePc is essentially the superposition of the spectra for the cast films of the neat components, as it occurred for LuPc<sub>2</sub>. However, the spectrum for the mixed LB film differs, which could be explained either by some molecular-level interaction between DMPA and FePc or by distinct molecular organizations of FePc in the films. Because no interaction was observed in the mixed Langmuir films, it seems that a change in organization is the most probable hypothesis.

The arrangement of the FePc molecules in the LB film may be determined considering the surface selection rules<sup>51,52</sup> according to which the intensity (*I*) of the absorption band is given by the scalar product between the dipole derivative ( $\mu'$ ) of the molecule and the electric field (*E*) of the incident radiation. As the incident IR beam is perpendicular to the substrate surface in the transmission mode, *E* is in a plane parallel to the substrate. Then, the vibrational modes with  $\mu'$  parallel to the surface are stronger in the transmission mode FTIR spectrum while those bands whose  $\mu'$  is perpendicular to the substrate tend to vanish. In a comparison with the spectrum for the cast mixed film, one notes that the spectrum for the mixed LB film is dominated by bands with  $\mu'$  in the plane of the FePc macrocycles, namely the bands at 1331 cm<sup>-1</sup> (stretching C=C or C=N (pyrrole), 1117 cm<sup>-1</sup> (in-plane C-H bending) and 1078 (in plane C-H or N-Fe bending, benzene deformation, CNC stretching).<sup>37,53-56</sup> In contrast, the relative intensity of the band at 730 cm<sup>-1</sup>, assigned to out-of-plane C-H wagging (*i.e.*, perpendicular to the FePc macrocycle), practically disappears. Therefore, one may conclude that FePc molecules are organized in the mixed LB films with the macrocycle preferentially normal to the substrate surface (edge-on orientation). It should be stressed that the arrangement of FePc molecules in thin films depends on the technique used to produce the films and on experimental parameters even using the same film preparation technique.<sup>45</sup>

## Electrochemical properties and sensitivity to catechol

### Bare ITO, ITO-cast films and ITO-LB films

The first step of the electrochemical study was to establish the electrochemical behavior of DMPA, FePc, LuPc<sub>2</sub>, and to analyze the effect from the presence of DMPA in mixtures of FePc + DMPA and LuPc<sub>2</sub> + DMPA. As it is not possible to obtain LB films of good quality of neat LuPc<sub>2</sub>, these preliminary studies were carried out in cast films. The results are presented in Fig. 5a (FePc, DMPA and FePc + DMPA) and Fig. 5b (LuPc<sub>2</sub>, DMPA and LuPc<sub>2</sub> + DMPA). The phospholipid DMPA does not exhibit redox activity, while the FePc has a reduction peak at -0.60 V assigned to the macrocycle ring<sup>57,58</sup> and the LuPc<sub>2</sub> has two redox pairs with the anodic peaks at 0.69 V and -0.16 V that are assigned to Ln(III)Pc<sub>2</sub>/Ln(III)Pc<sub>2</sub><sup>+</sup> and Ln(III)Pc<sub>2</sub>/Ln(III)Pc<sub>2</sub><sup>-</sup>, respectively.<sup>59</sup> The peak initially at -0.60 V for FePc is shifted to -0.77 V in the presence of DMPA (FePc + DMPA). For DMPA + LuPc<sub>2</sub>, the anodic peak associated with the oxidation of the Pc ring, initially at 0.69 V for LuPc<sub>2</sub>, is shifted to 0.64 V and the corresponding cathodic peak at 0.39 V is shifted to 0.45 V (see inset in Fig. 5b). The redox process with peaks at -0.16 V/-0.65 V is not affected by the presence of DMPA. It is worth mentioning that despite the shifts in the redox peaks for

the DMPA + LuPc<sub>2</sub> cast film, the *E*(1/2) values (0.54 V and -0.4 V) for both redox processes did not change significantly with DMPA. The latter corroborates the  $\pi$ -*A* isotherms and FTIR results in which there was no molecular-level interaction between LuPc<sub>2</sub> and DMPA. A strong similarity is noted between the voltammograms of the mixed cast films and those from the mixed LB films. This indicates that the molecular structure in the LB films does not modify the electrochemical properties of the materials.

### Kinetic studies

The voltammograms recorded using different scan rates, from 0.005 to 0.500 V s<sup>-1</sup>, for the LB films of FePc + DMPA and LuPc<sub>2</sub> + DMPA are shown in Fig. 6a and b, respectively. Linear plots of peak current (*i*<sub>pc</sub>) as a function of  $\nu^{1/2}$  were obtained in Fig. 6c for the reduction peak at -0.77 V for FePc + DMPA and at -0.89 V for LuPc<sub>2</sub> + DMPA, indicating that both processes are diffusion controlled. Also, the oxidation peak associated with this redox process at -0.37 V becomes evident only with higher scan rates. Nernstian processes were also observed for the peaks associated with the one electron oxidation of the LuPc<sub>2</sub> that appear at positive potentials. Because the angular coefficient of FePc + DMPA in Fig. 6c is higher than for LuPc<sub>2</sub> + DMPA, it is possible to infer that ion diffusion is faster for FePc + DMPA.

### Sensing properties

The sensing properties of the LB films were tested towards catechol, a diphenol of interest in the food industry. When analyzing a catechol solution using a bare ITO electrode as working electrode, a redox reactivity was observed with an intense anodic wave at 0.90 V and a cathodic peak at 0.05 V. Fig. 7a and b shows the cyclic voltammograms for the LB films of FePc + DMPA and LuPc<sub>2</sub> + DMPA as working electrodes. The voltammetric responses are dominated by an intense anodic peak associated with catechol that appears at 0.22 V for the FePc + DMPA film. This value is clearly lower than for bare ITO (0.90 V). The shift demonstrates the intense electrocatalytic activity caused by FePc at the electrode surface. The electrocatalytic effect is even more marked for the LuPc<sub>2</sub> + DMPA electrode, which lowers the oxidation potential of catechol to 0.14 V. In turn, the antioxidant activity of catechol causes a shift of the oxidation peak of LuPc<sub>2</sub> (initially at 0.72 V) to higher potentials and the peak can no longer be observed in the studied range.

The influence from the concentration of catechol in the voltammetric response was evaluated by obtaining voltammograms in catechol solutions from 3 to 144  $\mu$ M. The intensity of the oxidation-reduction peaks associated with catechol increased linearly with the antioxidant concentration. The detection limit (DL) and quantification limit (QL) were statistically calculated using  $DL = k \times SB/b$ , where *SB* is the standard deviation of the blank, *b* is the sensitivity of the method (determined as the slope of the calibration curve) and *k* is a statistical constant (values of 3 and 10 for DL and QL, respectively, are widely accepted).<sup>60</sup> Table 1 brings the values found for the sensitivity, DL and QL. Both mixed LB films present a linear trend at the analyzed concentration range ( $3 \times 10^{-6}$  to  $1.44 \times 10^{-4}$  M) with *R* = 0.999

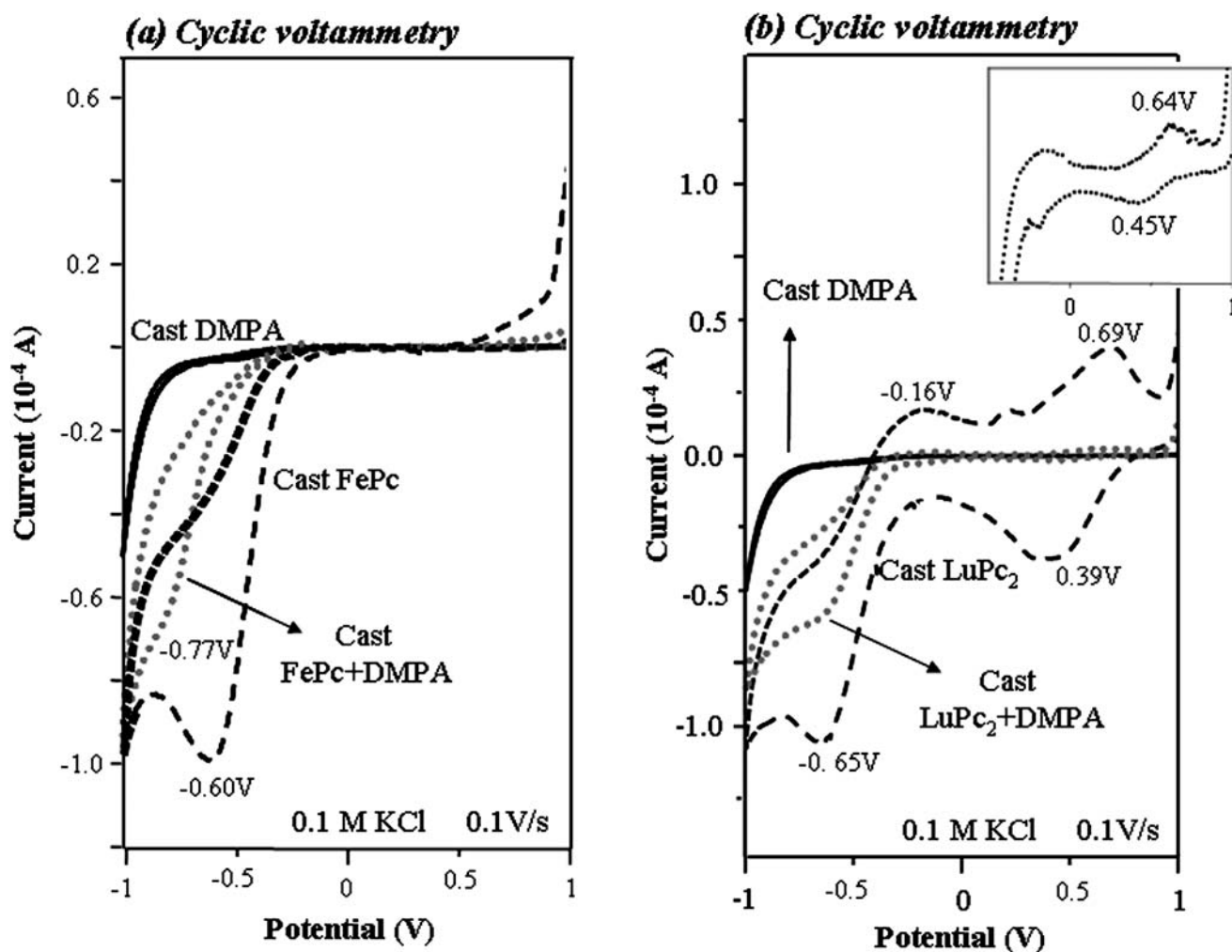


Fig. 5 Cyclic voltammograms recorded at 0.1 V s<sup>-1</sup> and 0.1 M KCl for cast films of (a) FePc, DMPA and FePc + DMPA and (b) LuPc<sub>2</sub>, DMPA and LuPc<sub>2</sub> + DMPA.

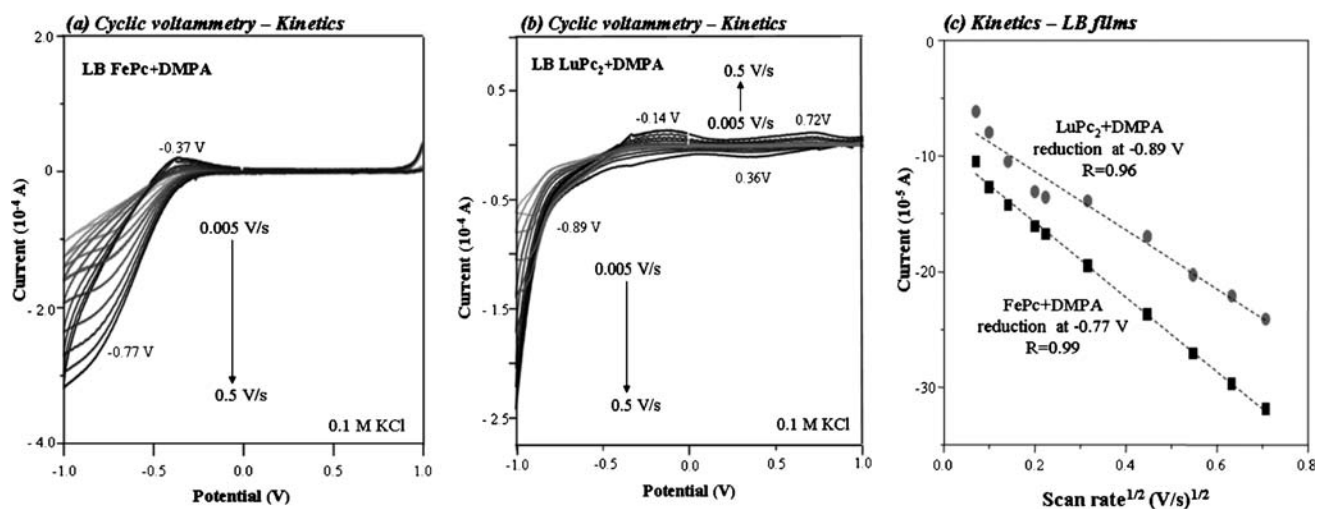
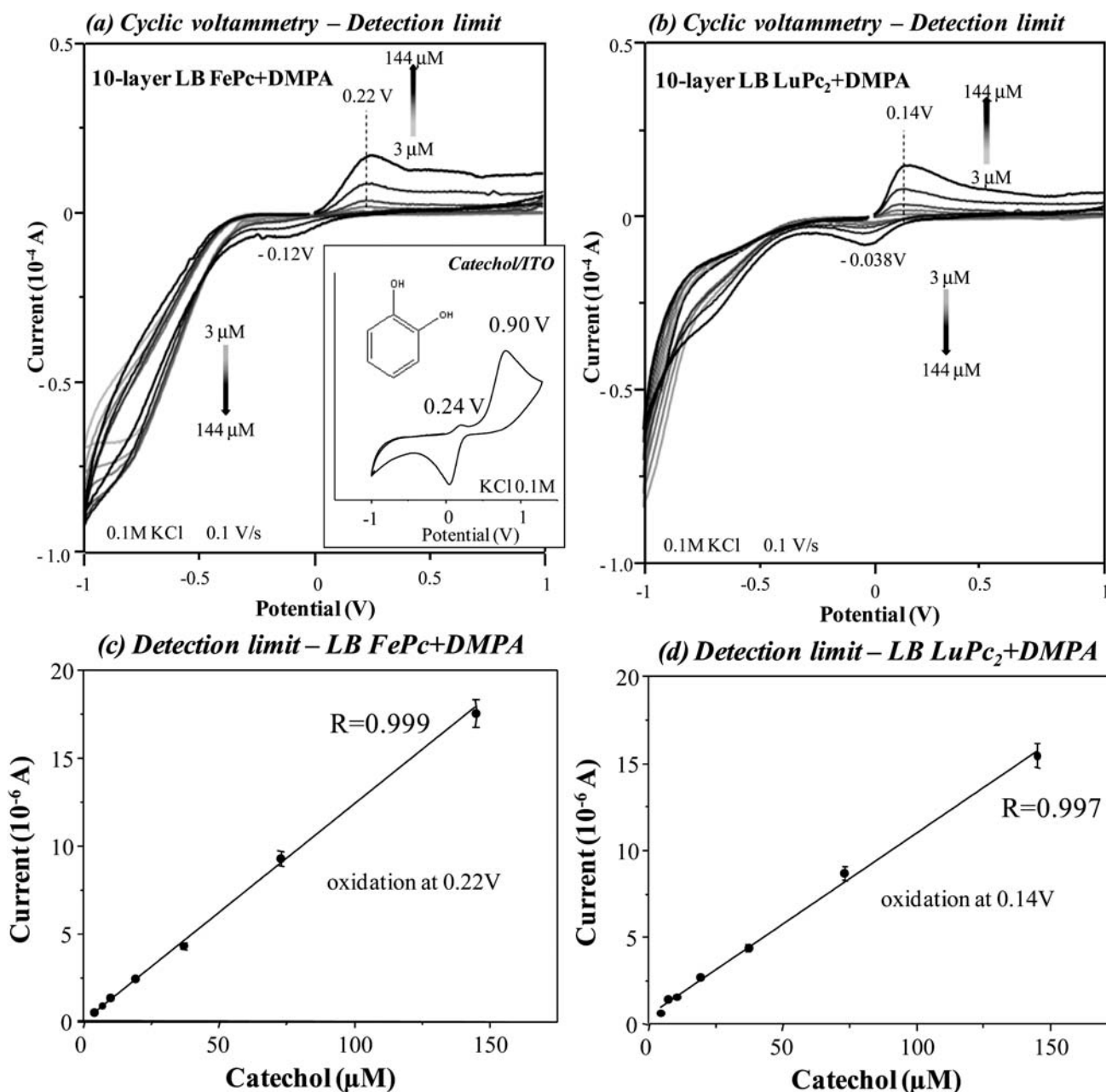


Fig. 6 Cyclic voltammograms recorded at different scan rates (0.005–0.5 V s<sup>-1</sup>) and 0.1 M KCl for mixed LB films of (a) FePc + DMPA and (b) LuPc<sub>2</sub> + DMPA. (c) Reduction peak intensities vs scan rate<sup>1/2</sup> for FePc + DMPA at -0.77 V and for LuPc<sub>2</sub> + DMPA at -0.89 V.



**Fig. 7** Cyclic voltammograms recorded at  $0.1 \text{ V s}^{-1}$ ,  $0.1 \text{ M KCl}$  and different concentrations of catechol ( $3\text{--}144 \mu\text{M}$ ) for mixed LB films of (a) FePc + DMPA and (b) LuPc<sub>2</sub> + DMPA. (c) Oxidation peak intensity vs catechol concentration for FePc + DMPA at  $0.22 \text{ V}$ . (d) Oxidation peak intensity vs catechol concentration for LuPc<sub>2</sub> + DMPA at  $0.14 \text{ V}$ . The error bars were estimated by taking the average of three measurements for each sample.

**Table 1** Sensitivity, detection limit (DL) and quantification limit (QL) for both mixed LB films in the presence of catechol ranging between  $3 \times 10^{-6}$  and  $1.44 \times 10^{-4} \text{ M}$

	LB FePc + DMPA	LB LuPc <sub>2</sub> + DMPA
Sensitivity/ $\mu\text{A } \mu\text{M}^{-1}$	1.21	1.04
Detection limit/ $\mu\text{M}$	0.430	0.334
Quantification limit/ $\mu\text{M}$	1.440	1.110

for FePc + DMPA and  $R = 0.997$  for LuPc<sub>2</sub> + DMPA. The sensitivity is comparable with detection limits for several similar sensors,<sup>61–69</sup> as demonstrated in Table 2. It has to be mentioned

that the DL in this work is higher than that of enzymatic biosensors (DL of  $3 \times 10^{-8} \text{ M}$ )<sup>70</sup> but has the advantage of the superior stability. Indeed, the films produced here could be cycled up to 500 times while sensors based on enzymes have an extremely short lifetime. Finally, the DL obtained for our sensors is in the range required by the food industry.

## Conclusions

We have shown that Langmuir films may be formed from bisphthalocyanines and phospholipids, and the mixture with DMPA allowed us to transfer LB films from LuPc<sub>2</sub>, which

**Table 2** List of references dealing with catechol detection using electrochemical method. Abbreviations: CPE—carbon paste electrode; MWNTs—multi-walled carbon nanotubes; P3MT—poly(3-methyl thiophene); GCE—glassy carbon electrode; SCE—saturated calomel electrode

Sensor	Electrochemical method	Potential/mV	Detection limit/ $\mu\text{M}$	Reference
Thionine-tyrosinase CPE	Amperometry	200 (Ag AgCl)	0.150	61
Electrosynthesized poly(aniline-co-p-aminophenol)	Amperometry	550 (SCE)	0.800	62
MWNTs/P3MT/GCE	DPV	203 (Ag AgCl)	0.050	63
N-Phenylethylene diamine methacrylamide—molecularly imprinted polymers	Cyclic voltammetry	0.35 V (Ag AgCl)	0.228	64
Screen printed graphite electrode	Square wave voltammetry	204 (SCE)	0.290	65
Mesoporous carbon CMK-3 modified electrode	Cyclic voltammetry	162 (SCE)	0.100	66
Enzyme-integrated carbon nanotube epoxy composite electrode (CNTEC-Tyr)	Amperometry	-200 (Ag AgCl)	10.000	67
Nylon-6 nanofibrous membrane based on tyrosinase biosensor	Amperometry	-200 (Ag AgCl)	0.050	68
Mesoporous Al-doped silica CPE	DPV	510 (SCE)	0.100	69

cannot form such films on its own, in spite of the absence of molecular-level interaction between the components. The mixed LB films showed a remarkable electrocatalytic effect that facilitated the oxidation of catechol, thus allowing its detection with a sensitivity ( $10^{-7}$  M) that is comparable to other non-enzymatic sensors, even without any optimization process. Using LB films was advantageous because of the higher stability, as observed in a comparative study with cast mixed films. This is promising for further studies as the LB films may serve as scaffolds for immobilization of enzymes, normally favored in phospholipid environments. Therefore, one may envisage a sensing system that may have its performance controlled by the molecular architecture of the film, especially with the supramolecular chemistry afforded by phthalocyanines (see Alencar *et al.*<sup>71</sup>). Studies on the nanostructuring of Langmuir and LB films and on the immobilization of enzymes are being conducted.

## Acknowledgements

The authors acknowledge FAPESP and CAPES (process 118/06) from Brazil and MICINN (PHB2005-0057-PC) and AGL2009-12660/ALI from Spain for the financial support.

## References

- 1 K. B. Blodgett, *J. Am. Chem. Soc.*, 1935, **57**, 1007.
- 2 M. C. Petty, *Langmuir–Blodgett Films: An Introduction*, Cambridge University Press, Cambridge, 1996.
- 3 K. Ariga, J. P. Hill, M. V. Lee, A. Vinu, R. Charvet and S. Acharya, *Sci. Technol. Adv. Mater.*, 2008, **9**, 014109.
- 4 G. Decher, J. D. Hong and J. Schmitt, *Thin Solid Films*, 1992, **210**, 831.
- 5 K. Ariga, J. P. Hill and Q. M. Ji, *Phys. Chem. Chem. Phys.*, 2007, **9**, 2319.
- 6 D. B. Mitzi, *Chem. Mater.*, 2001, **13**, 3283.
- 7 R. Kniprath, J. T. McLeskey, J. P. Rabe and S. Kirstein, *J. Appl. Phys.*, 2009, **105**, 124313.
- 8 H. Ohnuki, R. Honjo, H. Endo, T. Imakubo and M. Izumi, *Thin Solid Films*, 2009, **518**, 596.
- 9 K. Ariga, T. Nakanishi and T. Michinobu, *J. Nanosci. Nanotechnol.*, 2006, **6**, 2278.
- 10 Z. Matharu, S. K. Arya, S. P. Singh, V. Gupta and B. D. Malhotra, *Anal. Chim. Acta*, 2009, **634**, 243.
- 11 J. R. Siqueira, M. H. Abouzar, A. Poghossian, V. Zucolotto, O. N. Oliveira Jr and M. J. Schoning, *Biosens. Bioelectron.*, 2009, **25**, 497.
- 12 J. Cabaj, J. Soloduchko, A. Chyla, J. Bryjak and K. Zynek, *Sens. Actuators, B*, 2009, **136**, 425.
- 13 P. Wang, M. Liu and J. Q. Kan, *Sens. Actuators, B*, 2009, **140**, 577.
- 14 S. Abu Hanifah, L. Y. Heng and M. Ahmad, *Anal. Sci.*, 2009, **25**, 779.
- 15 D. Del Rio, L. G. Costa, M. E. J. Lean and A. Crozier, *Nutrition Metabolism and Cardiovascular Diseases*, 2010, **20**, 1.
- 16 F. Saura-Calixto and M. E. Díaz-Rubio, *Food Res. Int.*, 2007, **40**, 613.
- 17 T. Farooqui and A. A. Farooqui, *Mech. Ageing Dev.*, 2009, **130**, 203.
- 18 A. Moure, J. M. Cruz, D. Franco, J. M. Domínguez, J. Sineiro, H. Domínguez, M. J. Núñez and J. C. Parajó, *Food Chem.*, 2001, **72**, 145.
- 19 P. Chowdhury and T. Viraraghavan, *Sci. Total Environ.*, 2009, **40**, 2474.
- 20 C. A. Olivati, A. Riul Jr, D. T. Balogh, O. N. Oliveira Jr and M. Ferreira, *Bioprocess Biosyst. Eng.*, 2009, **32**, 41.
- 21 Y. Q. Zheng, C. Z. Yang, W. H. Pu and J. D. Zhang, *Microchim. Acta*, 2009, **166**, 21.
- 22 M. J. Klink and A. M. Crouch, *Microchim. Acta*, 2009, **166**, 27.
- 23 P. Dykstra, J. J. Hao, S. T. Koev, G. F. Payne, L. L. Yu and R. Ghodssi, *Sens. Actuators, B*, 2009, **138**, 64.
- 24 S. Bashir and J. L. Liu, *Sens. Actuators, B*, 2009, **139**, 584.
- 25 L. Caseli, A. C. Perinotto, T. Viitala, V. Zucolotto and O. N. Oliveira Jr, *Langmuir*, 2009, **25**, 3057.
- 26 W. J. R. Santos, A. L. Sousa, M. P. T. Sotomayor, F. S. Damos, S. M. C. N. Tanaka, L. T. Kubota and A. A. Tanaka, *J. Braz. Chem. Soc.*, 2009, **20**, 1180.
- 27 L. Ozcan, Y. Sahin and H. Turk, *Biosens. Bioelectron.*, 2008, **24**, 512.
- 28 Y. Liu, K. Shikahara and A. Yamada, *Thin Solid Films*, 1989, **179**, 303.
- 29 M. Linaje, M. C. Quintanilla, A. Gonzalez, J. L. Del Valle, G. Alcaide and M. L. Rodríguez-Méndez, *Analyst*, 2000, **125**, 341.
- 30 F. J. Pavinatto, L. Caseli, A. Pavinatto, D. S. Dos Santos Jr, T. M. Nobre, M. E. D. Zaniquelli, H. S. Silva, P. B. Miranda and O. N. Oliveira Jr, *Langmuir*, 2007, **23**, 7666.
- 31 L. Caseli, F. J. Pavinatto, T. M. Nobre, M. E. D. Zaniquelli, T. Viitala and O. N. Oliveira Jr, *Langmuir*, 2008, **24**, 4150.
- 32 R. C. Ahuja, P. L. Caruso, D. Mobius, G. Wildburg, H. Ringsdorf, D. Philp, J. A. Preece and J. F. Stoddart, *Langmuir*, 1993, **9**, 1534.
- 33 J. J. Giner-Casares, L. Camacho, M. T. Martín-Romero and J. J. L. Cascales, *Langmuir*, 2008, **24**, 1823.
- 34 Z. Wei, W. Xu, W. Hu and D. Zhu, *Langmuir*, 2009, **25**, 3349.
- 35 K. Ogawa, H. Yonehara and C. Pac, *Langmuir*, 1994, **10**, 2068.
- 36 A. Boguta, D. Wrobel, A. Bartczak, R. Swietlik, Z. Stachowiak and R. M. Ion, *Mater. Sci. Eng., B*, 2004, **113**, 99.
- 37 L. Gaffo, C. J. L. Constantino, W. C. Moreira, R. F. Aroca and O. N. Oliveira Jr, *Spectrochim. Acta, Part A*, 2004, **60**, 321.

- 38 R. E. Clavijo, D. Battisti, R. Aroca, G. J. Kovacs and C. A. Jennings, *Langmuir*, 1992, **8**, 113.
- 39 M. Maitrot, G. Guillaud, B. Boudjema, J. J. Andre, H. Strzelecka, J. Simon and R. Even, *Chem. Phys. Lett.*, 1987, **133**, 59.
- 40 J. Souto, L. Tomilova, R. Aroca and J. A. De Saja, *Langmuir*, 1992, **8**, 942.
- 41 M. Petty, D. R. Lovett, J. M. O'Connor and J. Silver, *Thin Solid Films*, 1989, **179**, 387.
- 42 T. Del Cano, R. Aroca, J. A. De Saja and M. L. Rodríguez-Méndez, *Langmuir*, 2003, **19**, 3747.
- 43 C. C. Leznoff and A. B. P. Lever, *Phthalocyanines Properties and Applications*, Wiley, Weinheim, 1989.
- 44 M. L. Rodríguez-Méndez, Y. Gorbunova and J. A. De Saja, *Langmuir*, 2002, **18**, 9560.
- 45 D. Volpati, P. Alessio, A. A. Zanolim, F. C. Storti, A. E. Job, M. Ferreira, A. Riul Jr, O. N. Oliveira Jr and C. J. L. Constantino, *J. Phys. Chem. B*, 2008, **112**, 15275.
- 46 H. L. Casal and H. H. Mantsch, *Biochim. Biophys. Acta*, 1984, **779**, 381.
- 47 P. Lozano, A. J. Fernandez, J. J. Ruiz, L. Camacho, M. T. Martin and E. Muñoz, *J. Phys. Chem. B*, 2002, **106**, 6507.
- 48 Y. Gorbunova, M. L. Rodríguez-Méndez, J. Souto, L. Tomilova and J. A. De Saja, *Chem. Mater.*, 1995, **7**, 1443.
- 49 R. Aroca, R. E. Clavijo, C. A. Jennings, G. J. Kovacs, J. M. Duff and R. O. Loutfy, *Spectrochim. Acta, Part A*, 1989, **45**, 957.
- 50 M. L. Rodríguez-Méndez, R. Aroca and J. A. De Saja, *Chem. Mater.*, 1993, **5**, 933.
- 51 M. K. Debe, *Prog. Surf. Sci.*, 1987, **24**, 1.
- 52 P. A. Antunes, C. J. L. Constantino, R. Aroca and J. Duff, *Appl. Spectrosc.*, 2001, **55**, 1341.
- 53 L. Gaffo, C. J. L. Constantino, W. C. Moreira, R. F. Aroca and O. N. Oliveira Jr, *Langmuir*, 2002, **18**, 3561.
- 54 R. Aroca and A. Thedchanamoorthy, *Chem. Mater.*, 1995, **7**, 69.
- 55 L. Gaffo, C. J. L. Constantino, W. C. Moreira, R. F. Aroca and O. N. Oliveira Jr, *J. Raman Spectrosc.*, 2002, **33**, 833.
- 56 Z. Liu, X. Zhang, Y. Zhang and J. Jiang, *Spectrochim. Acta, Part A*, 2007, **67**, 1232.
- 57 J. A. P. Chaves, M. F. A. Araújo, J. J. G. Varela and A. A. Tanaka, *Eclética Quím.*, 2003, **28**, 9.
- 58 P. Corio, J. C. Rubim and R. Aroca, *Langmuir*, 1998, **14**, 4162.
- 59 A. Arrieta, M. L. Rodríguez-Méndez and J. A. De Saja, *Sens. Actuators, B*, 2003, **95**, 357.
- 60 J. C. Miller and J. N. Miller, *Estadística para Química Analítica*, Addison-Wesley Iberoamericana, Delaware, 1993.
- 61 M. Portaccio, D. Di Tuoro, F. Arduini, M. Lepore, D. G. Mita, N. Diano, L. Mita and D. Moscone, *Biosens. Bioelectron.*, 2010, **25**, 2003.
- 62 C. Chen, C. Sun and Y. Gao, *Electrochim. Acta*, 2009, **54**, 2575.
- 63 H. Zhang, J. Zhao, H. Liu, R. Liu, H. Wang and J. Liu, *Microchim. Acta*, 2010, **169**, 277.
- 64 D. Lakshmi, A. Bossi, M. J. Whitcombe, I. Chianella, S. A. Fowler, S. Subrahmanyam, E. V. Piletska and S. A. Piletsky, *AnalChem*, 2009, **81**, 3576.
- 65 G. A. M. Mersal, *Int. J. Electrochem. Sci.*, 2009, **4**, 1167.
- 66 J. Yu, W. Du, F. Zhao and B. Zeng, *Electrochim. Acta*, 2009, **54**, 984.
- 67 B. P. Lopez and A. Merkoçi, *Analyst*, 2009, **134**, 60.
- 68 A. Arecchi, M. Scampicchio, S. Drusch and S. Mannino, *Anal. Chim. Acta*, 2010, **659**, 133.
- 69 H. Lin, T. Gan and K. Wu, *Food Chem.*, 2009, **113**, 701.
- 70 M. P. T. Sotomayor, A. A. Tanaka and L. T. Kubota, *Anal. Chim. Acta*, 2002, **455**, 215.
- 71 W. S. Alencar, F. N. Crespilho, M. V. A. Martins, V. Zucolotto, O. N. Oliveira Jr and W. C. Silva, *Phys. Chem. Chem. Phys.*, 2009, **11**, 5086.